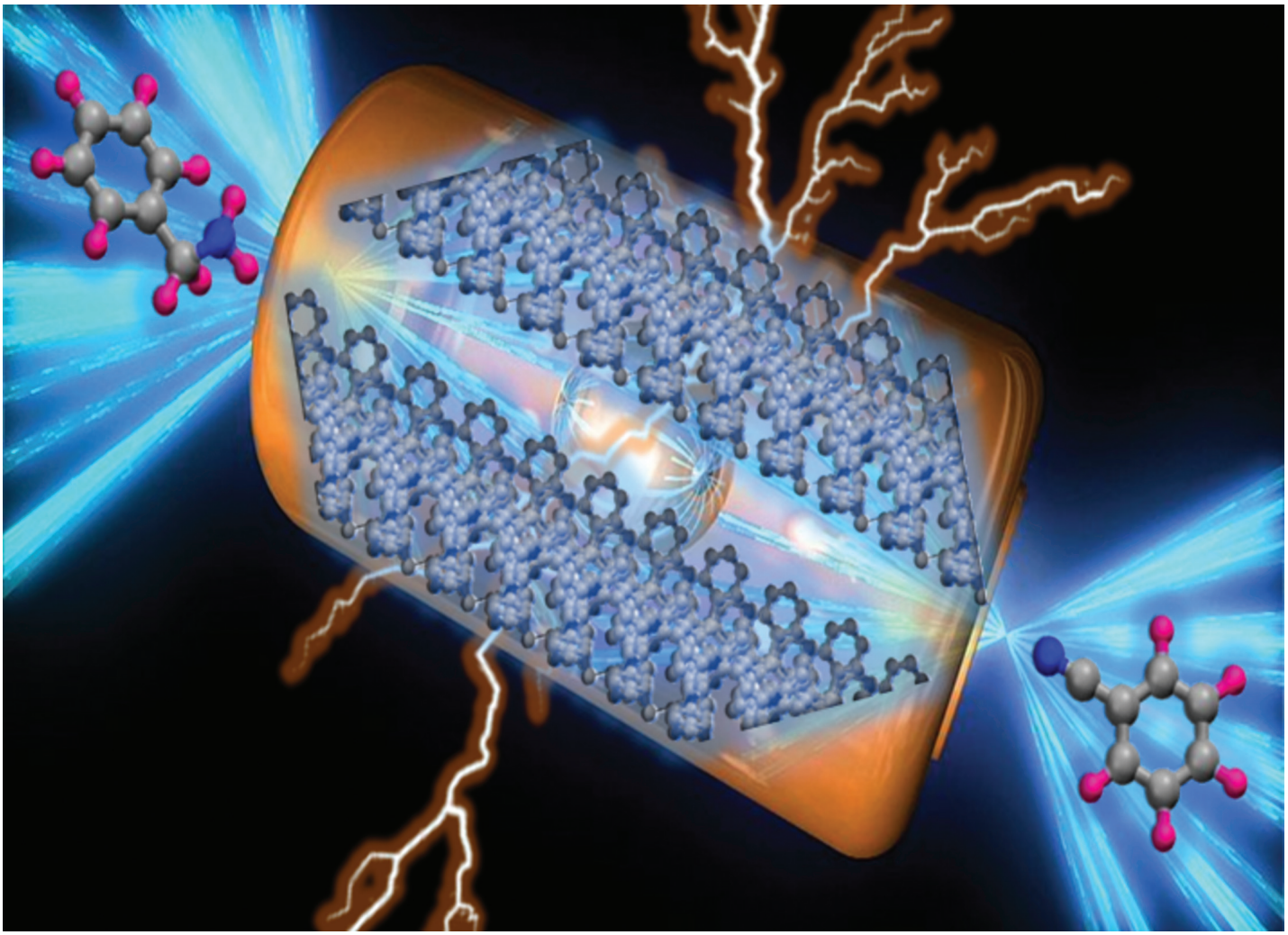

Showcasing research from Professor Gupta's laboratory, Department of Chemistry, University of Delhi, India.

Acceptorless oxidant-free dehydrogenation of amines catalyzed by Ru–hydride complexes of amide-acid/ester ligands

Acceptorless dehydrogenation of amines to nitriles and imines without using an oxidant or hydrogen acceptor is significant yet challenging. This work presents elegant Ru–hydride complexes illustrating oxidant-free, acceptorless, and selective dehydrogenation of both primary and secondary amines affording nitriles and imines, respectively. The catalytic activity is influenced by the associated multidentate ligand that creates hydrogen bonds to a substrate and aids in bringing it closer to the catalyst. Our results exquisitely exhibit that strategic ligand design can overcome challenges associated with oxidant-free and acceptorless dehydrogenation of amines.

Image reproduced by permission of Samanta Yadav and Rajeev Gupta from *Dalton Trans.*, 2025, **54**, 5675.

As featured in:

See Samanta Yadav and Rajeev Gupta, *Dalton Trans.*, 2025, **54**, 5675.

ROYAL SOCIETY OF CHEMISTRY

rsc.li/dalton

Registered charity number: 207890

Dalton Transactions

ROYAL SOCIETY OF CHEMISTRY

PAPER

View Article Online
View Journal | View Issue

Cite this: *Dalton Trans.*, 2025, **54**, 5675

Acceptorless oxidant-free dehydrogenation of amines catalyzed by Ru–hydride complexes of amide-acid/ester ligands†

Samanta Yadav and Rajeev Gupta *

Received 15th November 2024,
Accepted 7th February 2025

DOI: 10.1039/d4dt03201b

rsc.li/dalton

Traditional dehydrogenation of amines involves the transfer of hydrogen molecule(s) from a substrate to an acceptor. In acceptorless dehydrogenation, hydrogen gas is liberated without an oxidant, providing an efficient synthetic method. Acceptorless dehydrogenation of primary amines to nitriles without using an oxidant or hydrogen acceptor is significant yet challenging. Herein, we present efficient Ru-based catalysts capable of carrying out such a transformation with hydrogen gas as the only by-product. A new class of air and moisture-stable ruthenium–hydride complexes (**1–4**) of amide-acid/ester-based ligands have been synthesized and characterized. Crystal structures of two representative complexes, **2** and **3**, illustrate the bidentate N–O coordination mode of the ligands. At the same time, additional binding sites are occupied by one hydride, one CO, and two PPh_3 co-ligands. The catalytic behavior of these complexes is explored towards the oxidant-free, acceptorless, and selective dehydrogenation of primary and secondary amines affording nitriles and imines, respectively. Among four Ru(II) complexes, complex **2** showed the best catalytic activity for the dehydrogenation of amines. A wide variety of both primary and secondary amines were utilized to explore the substrate scope. The catalytic system tolerated both electron-withdrawing and electron-releasing substituents on amine substrates. Various control experiments and mechanistic studies were carried out to support the dehydrogenation of amines by using complex **2** as a representative catalyst.

Introduction

Nitriles are an eminent category of functional groups that are a part of multifaceted compounds involved in a wide variety of biologically active and industrial-relevant compounds.[1–3] Various methods have been employed to synthesize nitriles, but they suffer from poor atom economy, limited selectivity, use of noxious reagents, and harsh reaction conditions.[4] Typical synthetic methods include the cyanation of alkyl/aryl halides, dehydration of amides, metal-catalyzed cyanation, and Sandmeyer-type reactions.[5–9] On the other hand, industrial methods usually depend on the ammoxidation process that operates at high temperatures.[10] Most conventional methods for this transformation require an oxidant, which necessitates oxidant-compatible functional groups, thus significantly limiting the scope of amine oxidation reactions.[11–13]

An alternative synthetic method involves transition-metal-catalyzed double dehydrogenation of primary amines, considered one of the most suitable synthetic methods.[3,4,10,14,15] Although this method produces nitriles in excellent yields, many of such transition-metal catalyzed oxidation processes require large quantities of both oxidant and base for efficient catalytic conversion, which increases the amount of undesirable waste products while limiting the substrate scope for sensitive ones.[9,10,15] Nevertheless, double dehydrogenation of primary amines to nitriles is a noteworthy but demanding task as it involves the removal of two molecules of hydrogen while several competing pathways, such as coupling and transamination reactions, co-exist (Scheme 1).[3,9,16,17]

Till now, only a few examples are available in the literature for the selective, acceptorless, and oxidant-free dehydrogena-

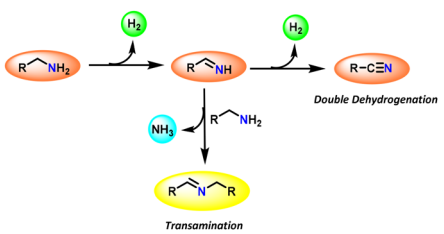

Scheme 1 Acceptorless double dehydrogenation of primary amines, including a competing coupling pathway.

Department of Chemistry, University of Delhi, Delhi-110 007, India.
E-mail: rgupta@chemistry.du.ac.in

†Electronic supplementary information (ESI) available. CCDC 2402741 and 2402742. For ESI and crystallographic data in CIF or other electronic format see DOI: https://doi.org/10.1039/d4dt03201b

tion of primary amines to nitriles. The first example was reported by Szymczak and co-workers in 2013 using (NNN)Ru–H complex as a catalyst (complex **a**, Scheme 2).[3] The authors proposed an inner-sphere mechanism that involved proton transfer from a coordinated amine to Ru–H followed by H_2 release.[18] Another example is an iridium–pincer complex, $[C_6H_3\text{-}2,6\text{-}(OP^tBu_2)_2IrH_2]$, which required a hydrogen acceptor and a base to afford nitrile products *via* an inner-sphere mechanism involving N–H oxidative addition followed by β-H elimination (complex **b**, Scheme 2).[19] An elegant Ru complex was reported by Bera and co-workers for an acceptorless dehydrogenation of primary amines to nitriles although it required the addition of a strong base to achieve the enhanced reactivity (complex **c**, Scheme 2).[14] Albrecht and co-workers have reported a pyridyl-triazole-based Ru–cymene complex which catalyzes the oxidation of both aromatic and aliphatic amines to nitriles using dioxygen as the terminal oxidant (complex **d**, Scheme 2).[15] Very recently, Tang and co-workers have proposed a tandem outer-sphere–inner-sphere mechanism using a Co catalyst (complex **e**, Scheme 2) for the dehydrogenation of amines *via* an imine intermediate.[4] However, due to limited examples of dehydrogenation of amine, it is still indistinct whether an inner-sphere, an outer-sphere, or a cooperative mechanism is dominant for such a double dehydrogenation process.[18]

Although these examples highlight the significance of acceptorless dehydrogenation of amines, harsh reaction conditions, including the strong bases, demand the development of newer catalysts.[4,14,20] Herein, we present Ru–hydride-based complexes for an acceptorless and oxidant-free dehydrogenation (DH) of amines. This work delineates the synthesis, characterization, and utilization of ruthenium complexes of pyridine–amide-based ligands for the catalytic conversion of amines to nitriles. The DH catalytic activity is found to be influenced by both the selection of a Ru(II) complex and the associated ligand. We show that an elegant ligand design can overcome challenges associated with acceptorless and oxidant-free DH of amines.

Results and discussion

Synthesis and characterization of ligands and their Ru(II) complexes

The amide-based ligands appended with ester (**HL1** and **HL3**) and carboxylic acid groups (**HL2** and **HL4**) were designed as viable hydrogen bond acceptors or donors to facilitate substrate binding and activation.[21,22] The ester–amide ligands **HL1** and **HL3** were synthesized by coupling 2-picolinic acid with 4-aminoethyl benzoate or 3-aminoethyl benzoate. The acid–amide-based ligands **HL2** and **HL4** were synthesized by the base-catalyzed hydrolysis of **HL1** and **HL3**, respectively. These ligands react with $[Ru(H)(Cl)(CO)(PPh_3)_3]$ in a MeOH–$CHCl_3$ mixture to form the corresponding [Ru–H] complexes **1–4** (Scheme 3). Both ligands and their Ru(II) complexes were thoroughly characterized using various spectroscopic techniques.

The CO stretching bands for complexes **1–4** were observed at 1921–1930 cm^{-1}.[23] The Ru–H signals were found to merge with the CO bands and appeared at 1957–1962 cm^{-1}.[24,25] The C═O group of ester in **1** and **3** were displayed at a higher wave number, *i.e.*, 1706 and 1709 cm^{-1}, compared to the acid group in **2** and **4**, which appeared at 1699 and 1697 cm^{-1}, respectively.[23] The amidic C═O bands for complexes **1–4** (1602–1610 cm^{-1}) were blue-shifted compared to the respective ligands (1575–1592 cm^{-1}) (Fig. S1–S8, ESI†). This advocates their coordination with the metal center (*vide infra*).[24,25] The amidic N–H stretches in ligands resonated at 3319–3342 cm^{-1}. These bands appeared even after metal complexation but were found red-shifted at 3225–3265 cm^{-1}. Such a fact suggests that a ligand binds with a Ru(II) ion through an amidic–O atom, subsequently confirmed by the X-ray crystallography (*vide infra*).

In the ^1H NMR spectra of Ru(II) complexes, the aromatic proton signals were shifted downfield compared to the ligands (Fig. S9–S16, ESI†). The signals for the N–H groups remain intact in **1–4** but were noted at higher δ values than their

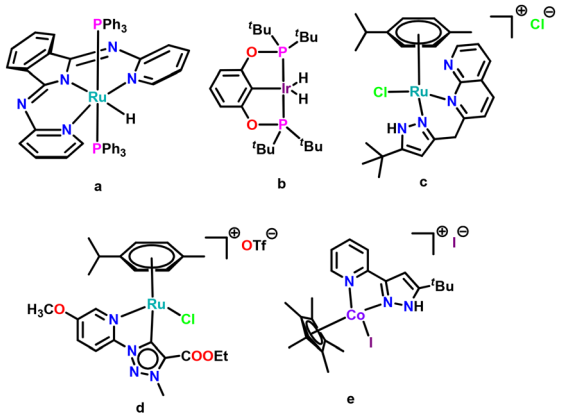

Scheme 2 Selected examples of metal complexes known for catalyzing the dehydrogenation of primary amines.

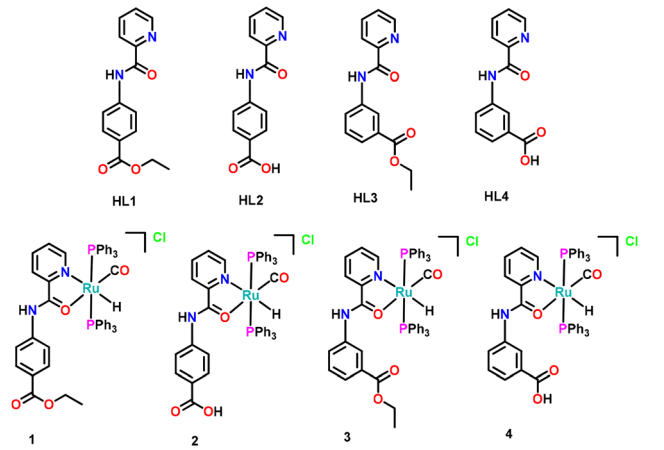

Scheme 3 Ligands HL1–HL4 and their Ru(II) complexes **1–4** discussed in this work.

corresponding ligands. For complexes **1–4**, the hydride signal appeared as a triplet at −10.27 ($J_{H,P}$ = 18.8 Hz), −10.23 ($J_{H,P}$ = 18.7 Hz), −10.20 ($J_{H,P}$ = 18.7 Hz), and −10.38 ppm ($J_{H,P}$ = 18.8 Hz), respectively.[26,27] The ^{13}C NMR spectra of complexes **1–4** showed CO group resonating at 203–211 ppm (Fig. S17–S24, ESI†). The ^{31}P NMR spectra for complexes **1–4** exhibited a singlet at 45.58–46.21 ppm (Fig. S25–S28, ESI†).[26,28] Such a fact asserted the presence of two PPh_3 groups *trans* to each other in a magnetically equivalent environment around a Ru center. The absorption spectra of complexes **1–4** exhibit bands at 415–435 nm and 300–305 nm, tentatively assigned to charge transfer and ligand-based transitions, respectively (Fig. S29, ESI†).[24,26] All ligands and their metal complexes were also characterized by the ESI$^+$ mass spectra (Fig. S30–S37, ESI†). The observed isotopic distribution pattern for complexes **1–4** matched excellently with the simulated patterns, while the most abundant peak was assigned to $[M - Cl]^+$ species.

To understand the redox behavior of Ru(II) complexes, cyclic voltametric studies were performed in DMF (Fig. S38, ESI†). The complexes **1–4** exhibited reductive responses in the negative potential region corresponding to Ru^{II}/Ru^{I} redox couple. For example, complexes **1** and **3** showed quasi-reversible reductive responses with $E_{1/2}$ at −1.84 V (ΔE = 130 mV) and −1.86 V (ΔE = 120 mV).[29] Both these complexes also displayed irreversible responses in the negative potential region with E_{pc} at −1.72 V and −1.70 V, assigned to ligand-based reductive events.[30] Similarly, complexes **2** and **4** exhibited quasi-reversible reductive responses at −1.90 V (ΔE = 90 mV) and −1.88 V (ΔE = 90 mV). Additionally, all four complexes showed irreversible oxidative responses with E_{pa} values of 1.39, 1.24, 1.42, and 1.29 V, respectively, corresponding to Ru^{III}/Ru^{II} redox event.[30]

Crystal structures

The structure and geometry of complexes **2** and **3** were confirmed with the help of the single crystal diffraction studies (Fig. 1 and Tables S1 and S2, ESI†). The molecular structures of complexes **2** and **3** displayed a distorted octahedral geometry around the Ru(II) center. The ligands acted as the bidentate entities, occupying two coordination sites, while the remaining sites were ligated by one hydride ion, one CO, and two PPh_3 groups.[25,27] Each Ru(II) ion was coordinated to two PPh_3 molecules, present *trans* to each other.[24,27] The P1–Ru–P2 bond angles for complexes **2** and **3** were 172.37(4) and 169.016(19)°, respectively.[26,27] The N1–Ru–H1 bond angles for both complexes were 165.9(9) and 174.2(6)°, signifying that the hydride ligand is located approximately at the *trans* position to that of the pyridyl ring. The CO ligand in both complexes was present at *trans* position to the amidic C═O group with bond angles of 172.64(17) and 173.49(7)°.[25–27] The Ru–PPh_3 bond lengths in both complexes were slightly longer than that of the Ru–H, Ru–CO, Ru–O_{amide}, and Ru–$N_{pyridine}$ bonds.[27] The Ru–O_{amide} and Ru–$N_{pyridine}$ bond lengths for **2** and **3** were 2.153(3) and 2.164(11) Å; and 2.176(3) and 2.174(15) Å, respectively. The Ru–O_{amide} bonds were relatively shorter when compared to the Ru–$N_{pyridine}$ bonds in both complexes. Such a fact indicates that the binding of the amidic–O was stronger than that of pyridyl–N.[25,27,31] In both complexes, one chloride ion was present outside the primary coordination sphere, which balanced the mono-cationic charge on the complexes.

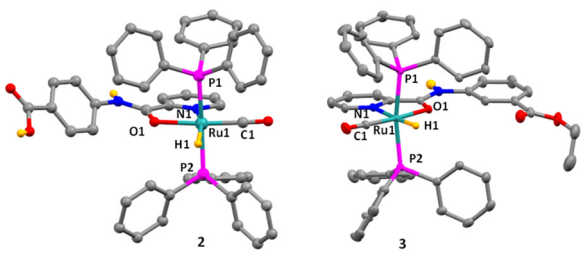

Fig. 1 Crystal structures of Ru(II) complexes **2** and **3**. Thermal ellipsoids are drawn at a 30% probability level, whereas selected hydrogen atoms have been shown for clarity.

Dehydrogenation of amines

Nitrile- and imine-containing compounds are considered significant as they are key building blocks for the synthesis of numerous organic compounds, including carboxylic acids, amides, amines, and heterocyclic compounds in addition to various industrially important products such as pharmaceuticals, dyes, pesticides, and polymers.[32] A noteworthy method for the preparation of nitriles is the oxidant-free and base-free dehydrogenation of amines catalyzed by transition metal complexes.[14,19] The dehydrogenation of amines has been very little investigated and documented, whereas the conventional methods involve the excessive use of bases, high temperatures, and hydrogen acceptors.[10,32] We have utilized the Ru–H complexes **1–4** for attempting DH of both primary and secondary amines to form nitriles and imines, respectively, generating hydrogen as the only by-product.

Initially, the reaction conditions for the acceptorless DH were optimized by taking benzylamine as a model substrate in toluene while using 2.0 mol% of complex **2** as a representative catalyst. This reaction resulted in 95% conversion to benzonitrile (Table 1). To examine the role of a catalyst, the DH reaction was performed in the absence of complex **2**, which did not result in any product formation (entry 1, Table 1). Two different Ru-precursors were employed to explore their catalytic efficiency; however, they only formed a negligible amount of the product (entries 2 and 3). The solvent screening was done using different solvents, such as dioxane, MeOH, DMF, CH_3CN, DCM, THF, and toluene (entry 4). The best DH result was obtained in toluene (entry 5). As the DH of amines requires higher temperatures, toluene expectedly provided the best result. The remaining Ru–H complexes were also utilized for the DH of benzylamine, resulting in comparatively lower product yield (entries 6–8). Notably, the best DH results were obtained with the amide–acid-based complexes **2** and **4**. We believe that the ability of the free –COOH group to form hydrogen bonds in these two complexes is a critical factor (*vide infra*).

Table 1 Optimization of reaction conditions for the acceptorless dehydrogenation of benzylamine[a]

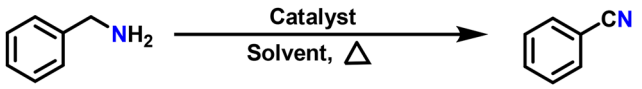

Entry	Catalyst	Solvent	Time (h)	Yield[b] (%)
1	—	Toluene	24	0
2	$[Ru(CO)_2Cl_2]_n$	Toluene	24	7
3	$RuH(CO)Cl(PPh_3)_3$	Toluene	24	5
4	**2**	Dioxane, MeOH, DMF, CH_3CN, DCM, THF	24	8, 0, 10, 4, 0, 0
5	**2**	**Toluene**	**24**	**95**
6	**1**	Toluene	24	90
7	**3**	Toluene	24	92
8	**4**	Toluene	24	93
9	**5**	Toluene	24	38
10[c]	**2**	Toluene	24	72
11	**2**	Toluene	12	52
12[d]	**2**	Toluene	24	65
13[e]	**2**	Toluene	24	78

[a] Reaction conditions: benzylamine (1.0 mmol), catalyst (2.0 mol%), solvent (5 mL), temperature (100 °C), time (24 h). [b] Determined by gas chromatography. [c] Catalyst (1.0 mol%). [d] 85 °C. [e] 90 °C.

Table 2 Acceptorless dehydrogenation of assorted primary amines catalyzed by complex **2** [a]

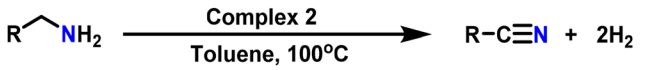

Entry	Substrate	Product	Yield[b] (%)
1	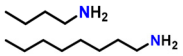	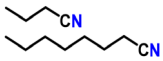	85
2	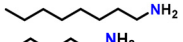		88
3	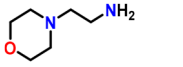	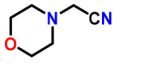	78
4	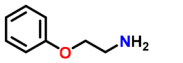	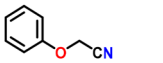	75
5	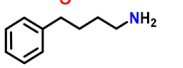	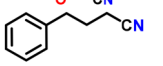	82
6	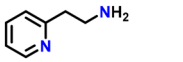	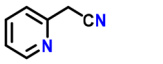	85
7	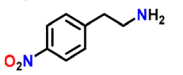	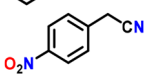	80

[a] Reaction conditions: amine (1.0 mmol), catalyst (2.0 mol%), toluene (5 mL), temperature (100 °C), time (24 h). [b] Yields were determined by gas chromatography. The selected products were characterized by ^1H NMR spectroscopy (Fig. S42–S45, ESI†).

Therefore, to substantiate the effect of the appended group on the catalytic activity, we synthesized a ruthenium complex, complex **5**, of the unsubstituted ligand. The complex **5** was characterized by ^1H, ^{13}C, and ^{31}P NMR spectra (Fig. S39–S41†). Subsequently, the catalytic activity of complex **5** was evaluated by carrying out DH of benzylamine. However, this complex was quite inferior in its catalytic activity and only resulted in a 38% yield of benzonitrile (entry 9; Table 1). It is, therefore, evident that the presence of an appended group in a ligand scaffold plays a vital role in DH catalysis, presumably due to its ability to form hydrogen bonds (*vide infra*).[33,34]

When the catalyst load is decreased (entry 10), the yield also decreases, and therefore, 2.0 mol% of a catalyst is ideal for the acceptorless DH of amines. The other reaction parameters, such as temperature and time, were also optimized (entries 11–13). The best reaction conditions for the acceptorless DH of benzylamine were as follows: 2.0 mol% complex **2** using toluene as a solvent at 100 °C for 24 h (entry 5). The homogeneity of the catalysis was established by performing the mercury drop and the 1,10-phenanthroline poisoning tests.[3] These studies did not result in any appreciable change in the product yield, thus confirming the homogeneity of DH.

After optimizing the reaction conditions, the substrate scope was extended for the acceptorless DH of assorted primary amines (Table 2). Double DH of butylamine and octylamine provided excellent yield of butyronitrile and octanenitrile, respectively (entries 1 and 2). Substrate 4-(2-aminoethyl) morpholine afforded a high yield of 2-morpholino-acetonitrile (entry 3). Similarly, 2-phenoxyethylamine, 4-phenyl-butylamine, 2-(2-pyridyl)ethylamine, and 2-(4-nitrophenyl) ethan-1-amine were converted to their corresponding nitriles in high yields (entries 4–7).

Subsequently, the substrate scope was extended to various aromatic primary amines (Table 3). As already discussed, double DH of benzylamine produced an excellent yield of benzonitrile (entry 1). The next aim was to study the effect of sterically and electronically distinct substituents on benzylamine.[3,14,15] The electron-donating groups, such as $-CH_3$, $-NH_2$, and –OH on benzylamine, afforded the corresponding substituted benzonitriles in excellent yields (entries 2–5).[14] The chemoselectivity was evaluated by carrying out the double DH of 2-aminobenzylamine and 4-aminobenzylamine, possessing both $-NH_2$ and $-CH_2NH_2$ functional groups (entries 3 and 4).[3] The exclusive formation of 2-aminobenzonitrile and 4-aminobenzonitrile confirmed the excellent chemoselectivity of the DH catalysis. Both these reactions adequately exemplify the advantages of opting for DH instead of conventional aerobic oxidation methods.[10,12,35] The benzylamines substituted with electron-withdrawing groups, such as –F, –Cl, –Br, and $-NO_2$, produced the respective benzonitriles in a slightly lower yield (entries 6–11).[3,14] Notably, heterocyclic aromatic amines also produced high yields of the corresponding nitriles, while the effect of a nitrogen atom's position in the ring was not pronounced (entries 12–14). Lastly, bulkier 1-naphthylmethylamine was efficiently converted to 1-naphthonitrile (entry 15).

After obtaining noteworthy results for the double DH of assorted primary amines, we explored the DH of secondary amines and other nitrogen-containing heterocycles (Table 4).[17,36] As per the literature, introducing a nitrogen atom in a cyclic system eases the DH process by lowering the

Table 3 Acceptorless dehydrogenation of assorted aromatic primary amines catalyzed by complex **2** [a]

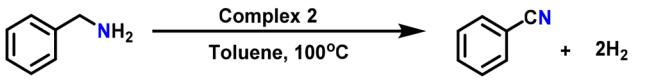

Entry	Substrate	Product	Yield[b] (%)
1	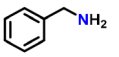		94
2	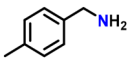	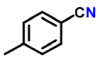	95
3	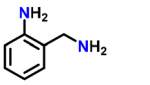		96
4	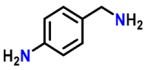	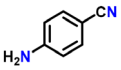	97
5	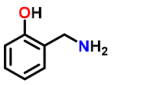		95
6	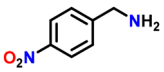	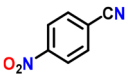	85
7	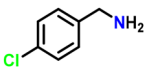	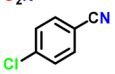	90
8	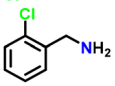		88
9	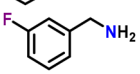	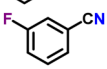	85
10	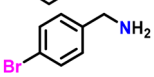	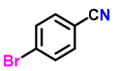	87
11	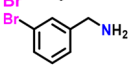	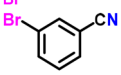	85
12	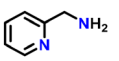		87
13	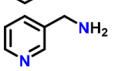		85
14	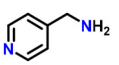		90
15	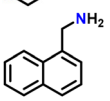		87

[a] Reaction conditions: amine (1.0 mmol), catalyst (2.0 mol%), toluene (5 mL), temperature (100 °C), time (24 h). [b] Yields were determined by gas chromatography. The selected products were characterized by ^{1}H NMR spectroscopy (Fig. S46–S60, ESI†).

Table 4 Acceptorless dehydrogenation of assorted secondary amines catalyzed by complex **2** [a]

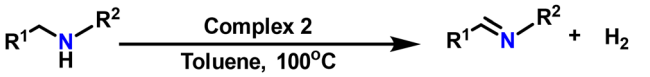

Entry	Substrate	Product	Yield[b] (%)
1			85
2			82
3	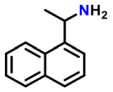		78
4	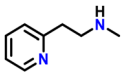	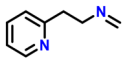	77
5			80
6			75
7			78

[a] Reaction conditions: amine (1.0 mmol), catalyst (2.0 mol%), toluene (5 mL), temperature (100 °C), time (24 h). [b] Yields were determined by gas chromatography. The selected products were characterized by ^{1}H NMR spectroscopy (Fig. S61–S63, ESI†).

catalytic reaction's endothermicity.[10] Gratifyingly, DH of 2-(methylamino)pyridine and 4-(methylamino)pyridine afforded good yields of *N*-(pyridin-2-yl)methanimine and *N*-(pyridin-4-yl)methanimine, respectively (entries 1 and 2). Further, 1-(naphthalen-1-yl)ethylamine and *N*-(2-(pyridin-2-yl)ethyl)ethanamine also produced respective imines in good yields (entries 3 and 4). Furthermore, DH of indoline yielded indole as the sole product (entry 5). Importantly, both *N*-benzylaniline and dibenzylamine afforded the respective dehydrogenated products in excellent yields (entries 6 and 7). These results assert both the high efficiency and selectivity of the present ruthenium hydride catalysts.[10,35] Although good selectivity and efficiency were achieved for the DH of secondary amines, the yield was comparatively lower than primary amines, most probably due to the presence of steric hindrance on the secondary amines.[10,32]

Binding and mechanistic studies

Binding and molecular docking studies were performed to get an insight into the mechanism of DH of amines. The binding ability of complex **2** towards benzylamine was investigated with the help of UV-Vis spectral titration in CH_3OH (Fig. 2a).[30,37,38] During the spectral titration, three isosbestic points were observed at 305, 320, and 420 nm, suggesting an interaction between complex **2** and benzylamine (Table S3 and Fig. S64†). The Job's plot suggested a 1 : 1 stoichiometry between complex **2** and benzylamine (Fig. 2b).[39] This fact was further supported by a linear regression fitting showing a 1 : 1 stoichiometry between complex **2** and benzylamine with a binding constant (K_b) of 1.23×10^3 M^{-1} (Fig. 2c).[30,38]

The molecular docking studies provided further evidence for the interaction of benzylamine with complex **2** (Fig. S65, Table S4, ESI†).[40] The docked structure exhibited that benzylamine interacts with complex **2** through a hydrogen bond between its $-NH_2$ group, and the –COOH group of the Ru–H complex. In addition, complex **2** showed dihydrogen bonding

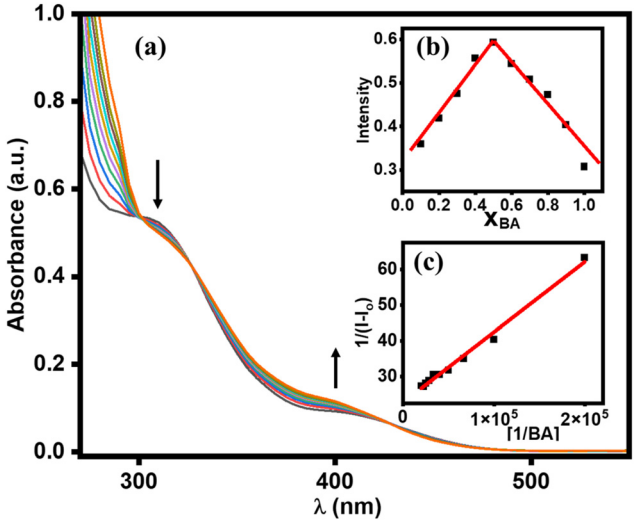

Fig. 2 (a) UV-Vis spectral titration of complex **2** (60 μM) with benzylamine (0–120 μM) in MeOH. Inset (b) Job's plot shows a 1 : 1 binding stoichiometry between **2** and benzylamine. Inset (c) linear regression fitting plot for a 1 : 1 binding stoichiometry between **2** and benzylamine. For both (b) and (c), spectral change at λ = 400 nm was monitored.

interaction with the –NH_2 group of benzylamine through its metal-bound hydride group. Furthermore, π···π stacking was also observed between one of the phenyl rings of the PPh_3 group of **2** to that of the arene ring of benzylamine.[37,38] All these interactions aided in bringing a substrate (*i.e.*, benzylamine) closer to the catalyst (*i.e.*, complex **2**) and assisted in DH catalysis.[37]

The proton NMR spectrum of a 1 : 1 mixture of complex **2** and benzylamine was measured to further substantiate binding and molecular docking studies. The ^{1}H NMR spectrum of this mixture exhibited notable shifts in the signals compared to the proton NMR spectrum of only complex **2** (Fig. S66, ESI†). The Ru–H signal was also found to shift from −10.35 to −10.31 ppm. Collectively, all studies attributed that a molecule of benzylamine was held in place by the involvement of various hydrogen bonding and π···π interactions, as illustrated by the molecular docking studies.

Based on all experiments and literature reports, a tentative mechanism is proposed for the acceptorless double DH of benzylamine as a representative substrate (Scheme S1, ESI†). In the first step, a molecule of benzylamine interacts with the catalyst through hydrogen bonding and π···π stacking to generate species **A**. It is worth mentioning that binding, molecular docking, and proton NMR spectral studies have provided evidence for this step (Scheme 4). This step was followed by the irreversible release of the first molecule of H_2, leading to the generation of intermediate **B**. Intermediate **B** undergoes β-hydride elimination to form the Ru–imine intermediate **C**. The next step is the irreversible release of a second molecule of H_2 to form the species **D**. Finally, a molecule of PPh_3 replaces benzonitrile as the final product, thus completing the catalytic cycle. The formation of the imine intermediate was not detected in the reaction mixture, indicating that the release of the second molecule of H_2 is fast. Importantly, the release of two equiv. of H_2 was quantified using a gas burette apparatus, while its detection was ascertained with the help of gas chromatography. Such a fact supports the proposed mechanism.[14]

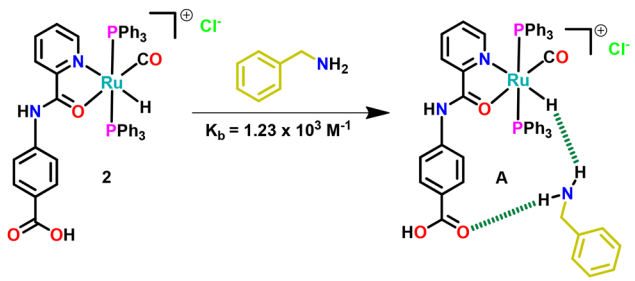

Scheme 4 The proposed binding interactions between complex **2** and a molecule of benzylamine.

Conclusions

A new class of ruthenium hydride complexes supported with pyridine–amide-based ligands containing appended ester and/or acid groups was presented. All Ru(II) complexes were thoroughly characterized using various spectroscopic techniques, while crystal structures were obtained for a few representative cases. The catalytic behavior of these Ru–H complexes was explored for the oxidant-free and acceptorless dehydrogenation of both primary and secondary amines to nitriles and imines, respectively. These Ru–H complexes supported a wide substrate scope and operated under mild reaction conditions. These ruthenium catalysts tolerated both electron-withdrawing and electron-releasing groups present on a substrate. Various control experiments and mechanistic studies supported the mechanism for the dehydrogenation of amines catalyzed by the ruthenium hydride complexes. These results elegantly illustrate that strategic ligand design can overcome challenges associated with oxidant-free and acceptorless dehydrogenation of amines.

Experimental

Materials

All reagents and chemicals were procured from commercial sources and used without further purification. The solvents were dried and/or purified using the standard literature procedures.[41] Precursor [Ru(H)(Cl)(CO)(PPh_3)$_3$] was prepared according to a reported literature method.[29]

Synthesis of ligands

Ethyl 4-(picolinamido)benzoate (HL1). 2-Picolinic acid (1.00 g, 8.13 mmol) was added as a solid to a suspension of ethyl-4-aminobenzoate (1.34 g, 8.13 mmol) in pyridine (10 mL)

and the mixture was stirred at 70 °C for 30 min. After that, triphenylphosphite (1.26 g, 8.13 mmol) was added drop-wise over 10 min. The temperature of the mixture was increased to 85 °C and the reaction was stirred for the next 8 h. Under reduced pressure, the solvent was removed, and a white product was obtained by washing the mixture several times with cold water. This product was further purified by recrystallization from CH_3OH. Yield: 2.05 g, 93%. Anal. calcd for $C_{15}H_{14}N_2O_3$: C, 66.66%; H, 5.22%; N, 10.36%. Found: C, 66.74%; H, 5.67%; N, 10.53%. FTIR spectrum (diamond ATR, cm^{-1}): 3319, 1706, 1608, 1523, 1404, 1266, 1101, 771, 682. ^{1}H NMR spectrum (400 MHz, $CDCl_3$, 25 °C) δ (ppm) 10.20 (s, 1H), 8.60 (d, J = 4.8 Hz, 1H), 8.28 (d, J = 7.8 Hz, 1H), 8.06 (d, J = 8.7 Hz, 2H), 7.90 (t, J = 7.7 Hz, 1H), 7.85 (d, J = 8.8 Hz, 2H), 7.49 (dd, J = 8.2, 4.2 Hz, 1H), 4.35 (q, J = 7.1 Hz, 2H), 1.38 (t, J = 7.1 Hz, 3H). ^{13}C NMR spectrum (100 MHz, $CDCl_3$, 25 °C) δ (ppm) 166.27, 162.30, 149.39, 148.13, 141.82, 137.91, 130.95, 126.88, 126.06, 122.62, 118.92, 60.96, 14.46. MS spectrum (ESI^+, MeOH): m/z calcd for $C_{15}H_{14}N_2O_3$ [M + H^+] 271.1004, found: 271.1080.

4-(Picolinamido)benzoic acid (HL2). The ligand H**L2** was obtained after the base-catalyzed hydrolysis of ligand H**L1**. H**L1** (1.00 g, 3.70 mmol) was dissolved in a mixture of THF : H_2O (3 : 1, v/v) and treated with 2 equivalents of NaOH. The reaction mixture was stirred for 12 h at room temperature. The resulting solution was neutralized by 4 N HCl and the mixture was stirred for 1 h. After removal of THF under vacuum white precipitates of H**L2** appeared that were filtered under suction. Yield: 0.82 g (87%). Anal. calcd for $C_{13}H_{10}N_2O_3$: C, 64.46%; H, 4.16%; N, 11.56%. Found: C, 64.92%; H, 4.77%; N, 12.03%. FTIR spectrum (diamond ATR, cm^{-1}): 3325, 1685, 1606, 1525, 1431, 1284, 1109, 769, 678. ^{1}H NMR spectrum (400 MHz, DMSO-d_6, 25 °C) δ (ppm) 12.74 (s, 1H), 10.87 (s, 1H), 8.71 (d, J = 4.6 Hz, 1H), 8.14 (d, J = 7.8 Hz, 1H), 8.08–7.97 (m, 3H), 7.90 (d, J = 8.7 Hz, 2H), 7.65 (dd, J = 6.3, 4.8 Hz, 1H). ^{13}C NMR spectrum (100 MHz, DMSO-d_6, 25 °C) δ (ppm) 167.46, 163.48, 150.10, 149.03, 142.95, 138.76, 130.74, 127.72, 126.30, 123.15, 120.15. MS spectrum (ESI^+, MeOH): m/z calcd for $C_{15}H_{14}N_2O_3$ [M + H^+] 243.0691, found: 243.0767.

Ethyl 3-(picolinamido)benzoate (HL3). The ligand H**L3** was synthesized in a similar manner with the same scale as that of H**L1** by using 2-picolinic acid (1.00 g, 8.13 mmol) and ethyl-3-aminobenzoate (1.34 g, 8.13 mmol). Yield: 1.97 g (89%). Anal. calcd for $C_{15}H_{14}N_2O_3$: C, 66.66%; H, 5.22%; N, 10.36%. Found: C, 66.87%; H, 5.42%; N, 10.33%. FTIR spectrum (diamond ATR, cm^{-1}): 3333, 1703, 1610, 1539, 1438, 1288, 1116, 765, 657. ^{1}H NMR spectrum (400 MHz, $CDCl_3$, 25 °C) δ (ppm) 10.12 (s, 1H), 8.60 (d, J = 7.2 Hz, 1H), 8.33–8.21 (m, 2H), 8.16 (d, J = 8.1 Hz, 1H), 7.90 (t, J = 7.7 Hz, 1H), 7.81 (d, J = 7.7 Hz, 1H), 7.47 (dt, J = 15.9, 5.8 Hz, 2H), 4.38 (q, J = 7.1 Hz, 2H), 1.39 (t, J = 7.1 Hz, 3H). ^{13}C NMR spectrum (100 MHz, $CDCl_3$, 25 °C) δ (ppm) 166.33, 162.28, 149.51, 148.14, 137.90, 131.41, 129.25, 126.78, 125.43, 124.03, 122.53, 120.66, 61.24, 14.45. MS spectrum (ESI^+, MeOH): m/z calcd for $C_{15}H_{14}N_2O_3$ [M + H^+] 271.1004, found: 271.1080.

3-(Picolinamido)benzoic acid (HL4). The ligand H**L4** was synthesized from H**L3** (1.00 g, 3.70 mmol) using a similar method as explained for H**L2**. Yield: 0.76 g (81%). Anal. calcd for $C_{13}H_{10}N_2O_3$: C, 64.46%; H, 4.16%; N, 11.56%. Found: C, 65.02%; H, 4.56%; N, 11.74%. FTIR spectrum (diamond, cm^{-1}): 3342, 1670, 1602, 1533, 1440, 1296, 1130, 752, 624. ^{1}H NMR spectrum (400 MHz, DMSO-d_6, 25 °C) δ (ppm) 12.95 (s, 1H), 10.81 (s, 1H), 8.71 (d, J = 4.7 Hz, 1H), 8.58 (s, 1H), 8.13 (d, J = 7.8 Hz, 1H), 8.04 (dd, J = 7.7, 5.9 Hz, 2H), 7.65 (dd, J = 9.5, 6.1 Hz, 2H), 7.44 (t, J = 7.9 Hz, 1H). ^{13}C NMR spectrum (100 MHz, DMSO-d_6, 25 °C) δ (ppm) 167.74, 163.36, 150.28, 149.00, 139.17, 131.79, 129.40, 127.57, 125.23, 125.18, 123.04, 121.64. MS spectrum (ESI^+, MeOH): m/z calcd for $C_{15}H_{14}N_2O_3$ [M + H^+] 243.0691, found: 243.0774.

Synthesis of Ru(II) complexes

[Ru(HL^1)(CO)(H)(PPh_3)$_2$] (1). A suspension of [Ru(H)(Cl)(CO)(PPh_3)$_3$] (0.100 g, 0.10 mmol) in 20 mL CH_3OH/$CHCl_3$ (1 : 1) mixture was treated with ligand H**L1** (0.0284 g, 0.10 mmol) and refluxed at 65 °C for 6 h which resulted in a yellow-colored solution. After completion of the reaction, volume was reduced to one-third using a rotary evaporator, and diethyl ether was added until the precipitation was complete. The product was then collected by filtration and dried under vacuum. Single crystals suitable for X-ray analysis were obtained by the vapor diffusion of diethyl ether into a saturated methanol–chloroform solution of the complex. Yield: 0.088 g (90%). Anal. calcd for $C_{52}H_{45}N_2O_4P_2ClRu$: C 65.03, H 4.72, N 2.92; found: C 65.55, H 5.12, N 3.33. FTIR spectrum (diamond, cm^{-1}): 1957, 1923, 1706, 1597, 1431, 1271, 1055, 696, 509. UV/Vis spectrum (MeOH, λ_{max}, nm): 300, 435. ^{1}H NMR spectrum (400 MHz, $CDCl_3$, 25 °C) δ (ppm) 8.20 (d, J = 5.3 Hz, 1H), 7.91 (d, J = 7.8 Hz, 1H), 7.44 (t, J = 7.6 Hz, 2H), 7.36–7.30 (m, 11H), 7.19 (dd, J = 11.9, 4.6 Hz, 8H), 7.07 (t, J = 7.6 Hz, 12H), 6.46–6.36 (m, 1H), 6.20 (d, J = 8.7 Hz, 2H), 4.27 (q, J = 7.2 Hz, 2H), 1.33 (t, J = 7.1 Hz, 3H). ^{13}C NMR spectrum (100 MHz, $CDCl_3$, 25 °C) δ (ppm) 211.37, 180.70, 167.48, 151.43, 146.69, 137.12, 135.81, 133.27, 132.10, 131.87, 130.2, 128.47, 127.99, 126.93, 126.19, 123.81. ^{31}P NMR (160 MHz, $CDCl_3$, 25 °C) δ (ppm) 46.21. MS spectrum (ESI^+, MeOH): m/z calcd for $C_{52}H_{45}N_2O_4P_2Ru$ [M − Cl]$^+$ 925.1898, found: 925.1894.

[Ru(HL^2)(CO)(Cl)(PPh_3)$_2$] (2). This product was prepared according to the same procedure as mentioned for complex **1** using the following reagents: [Ru(H)(Cl)(CO)(PPh_3)$_3$] (0.100 g, 0.10 mmol) and H**L2** (0.0252 g, 0.10 mmol). Yield: 0.090 g (93%). Anal. calcd for $C_{50}H_{41}N_2O_4P_2ClRu$: C 64.41, H 4.43, N 3.80; found: C 64.68, H 4.87, N 3.99. FTIR spectrum (diamond, cm^{-1}): 1921, 1699, 1575, 1554, 1174, 1091, 694, 509. UV/Vis spectrum (MeOH, λ_{max}, nm): 304, 420. ^{1}H NMR spectrum (400 MHz, $CDCl_3$, 25 °C) δ (ppm) 9.52 (s, 1H), 7.91 (d, J = 7.8 Hz, 1H), 7.86 (d, J = 5.0 Hz, 1H), 7.71 (s, 1H), 7.55 (d, J = 8.3 Hz, 2H), 7.47 (dd, J = 12.0, 5.6 Hz, 1H), 7.29 (dd, J = 13.6, 7.2 Hz, 9H), 7.22 (t, J = 7.7 Hz, 7H), 6.87–6.82 (m, 15H), −10.23 (t, J = 18.7 Hz, 1H). ^{13}C NMR spectrum (100 MHz, DMSO-d_6, 25 °C) δ (ppm): 203.37, 167.39, 163.43, 150.06, 148.99, 142.88, 138.70, 134.91, 134.34, 133.33, 132.00, 130.60, 129.07, 128.57, 127.66, 123.08. ^{31}P NMR (160 MHz, DMSO-d_6, 25 °C) δ (ppm)

45.58. MS spectrum (ESI^+, MeOH): *m*/*z* calcd for $C_{50}H_{41}N_2O_4P_2Ru$ $[M - Cl]^+$ 897.1585, found: 897.1577.

$[Ru(HL^3)(CO)(Cl)(PPh_3)_2]$ (3). Complex **3** was synthesized by using the same procedure as described for complex **1** starting from $[Ru(H)(Cl)(CO)(PPh_3)_3]$ (0.100 g, 0.10 mmol) in 20 mL $CH_3OH/CHCl_3$ (1 : 1) mixture with ligand H**L3** (0.0284 g, 0.10 mmol). Yield: 0.086 g (88%). Anal. calcd for $C_{52}H_{45}N_2O_4P_2ClRu$: C 65.03, H 4.72, N 2.92; found: C 65.43, H 4.92, N 3.12. FTIR spectrum (diamond, cm^{-1}): 3365, 1971, 1930, 1709, 1592, 1438, 1263, 1093, 752, 690. UV/Vis spectrum (MeOH, λ_{max}, nm): 305, 416. ^1H NMR spectrum (400 MHz, $CDCl_3$, 25 °C) δ (ppm) 12.49 (s, 1H), 9.63 (d, J = 8.0 Hz, 1H), 8.43 (s, 1H), 7.85 (d, J = 7.8 Hz, 2H), 7.76 (d, J = 5.2 Hz, 1H), 7.71 (t, J = 7.9 Hz, 1H), 7.47 (dd, J = 12.3, 5.4 Hz, 12H), 7.29 (dd, J = 11.0, 7.5 Hz, 5H), 7.20 (t, J = 7.3 Hz, 12H), 6.83–6.77 (m, 1H), 4.44 (q, J = 7.1 Hz, 2H), 1.43 (t, J = 7.1 Hz, 3H), −10.20 (t, J = 18.7 Hz, 1H). ^{13}C NMR spectrum (100 MHz, $CDCl_3$, 25 °C) δ (ppm): 167.90, 151.48, 137.15, 136.36, 133.31, 132.07, 131.74, 131.54, 128.64, 124.11, 14.59. ^{31}P NMR (160 MHz, $CDCl_3$, 25 °C) δ (ppm) 46.17. MS spectrum (ESI^+, MeOH): *m*/*z* calcd for $C_{52}H_{45}N_2O_4P_2Ru$ $[M - Cl]^+$ 925.1898, found: 925.1942.

$[Ru(HL^4)(CO)(Cl)(PPh_3)_2]$ (4). A similar method as mentioned for complex **1** was adopted using $[Ru(H)(Cl)(CO)(PPh_3)_3]$ (0.100 g, 0.10 mmol) and H**L4** (0.0252 g, 0.10 mmol). Yield: 0.084 g (87%). Anal. calcd for $C_{50}H_{41}N_2O_4P_2ClRu$: C 64.41, H 4.43, N 3.80; found: C 64.77, H 4.69, N 4.05. FTIR spectrum (diamond, cm^{-1}): 3332, 1990, 1928, 1697, 1577, 1442, 1207, 1093, 750, 660. UV/Vis spectrum (MeOH, λ_{max}, nm): 302, 415. ^1H NMR spectrum (400 MHz, $CDCl_3$, 25 °C) δ (ppm) 12.32 (s, 1H), 10.17 (s, 1H), 9.58 (s, 2H), 8.44 (s, 1H), 8.37–8.26 (m, 3H), 7.94 (d, J = 7.7 Hz, 5H), 7.71 (d, J = 7.4 Hz, 3H), 7.49 (d, J = 5.2 Hz, 10H), 7.23 (d, J = 6.7 Hz, 14H), −10.13 (d, J = 18.6 Hz, 1H). ^{13}C NMR spectrum (100 MHz, $CDCl_3$, 25 °C) δ (ppm) 166.17, 151.43, 137.82, 137.24, 136.28, 133.65, 133.17, 132.30, 131.76, 130.29, 128.58. ^{31}P NMR (160 MHz, $CDCl_3$, 25 °C) δ (ppm) 45.65. MS spectrum (ESI^+, MeOH): *m*/*z* calcd for $C_{50}H_{41}N_2O_4P_2Ru$ $[M - Cl]^+$ 897.1585, found: 897.1632.

Complex 5. A similar method as mentioned for complex **1** was adopted using $[Ru(H)(Cl)(CO)(PPh_3)_3]$ (0.100 g, 0.10 mmol) and the unsubstituted ligand (0.0198 g, 0.10 mmol). Yield: 0.072 g (81%). ^1H NMR spectrum (400 MHz, $CDCl_3$, 25 °C) δ (ppm) 12.42 (s), 9.53 (d, J = 7.9 Hz), 7.84 (d, J = 5.2 Hz), 7.68 (t, J = 7.6 Hz), 7.46 (dt, J = 14.9, 7.3 Hz), 7.27 (d, J = 7.2 Hz), 7.20 (t, J = 7.3 Hz), 6.81 (dd, J = 7.1, 5.6 Hz), −10.26 (t, J = 18.9 Hz). ^{13}C NMR spectrum (100 MHz, $CDCl_3$, 25 °C) δ (ppm) 208.00, 167.51, 151.58, 146.83, 144.64, 137.24, 135.90, 133.33, 132.01, 131.74, 130.23, 129.40, 128.44, 127.73, 126.23, 123.72. ^{31}P NMR (160 MHz, $CDCl_3$, 25 °C) δ (ppm) 46.21.

Typical procedure for the dehydrogenation of amines

An amine substrate (1.00 mmol) was added to a 10 mL round bottom flask containing a solution of complex **2** (2.0 mol%) in toluene (5 mL). The round bottom flask was capped with a septum and then heated to 100 °C under N_2 atmosphere. The progress of the reaction was monitored by thin-layer chromatography (TLC). After 24 h, the reaction mixture was cooled, and the solvent was evaporated under reduced pressure. The residue was dissolved in ethyl acetate, and yield was determined by gas chromatography. The products were purified by the silica gel chromatography using hexanes : ethyl acetate (3 : 1) mixture which afforded the corresponding nitrile as the isolated product. The identity and the purity of the nitrile products were confirmed by a combination of GC and NMR spectral techniques. As control and optimization experiments used benzylamine as a reactant that produces benzonitrile as a product on DH, so, the calibration plot was studied for this reactant/product combination (Fig. S67, ESI†).

Estimation of evolved H_2 during the dehydrogenation of benzylamine

Benzylamine (1.00 mmol) was added to a 10 mL round bottom flask containing a solution of complex **2** (2.0 mol%) in toluene (5 mL) and heated to 100 °C. The round bottom flask was connected to a gas burette apparatus through a cold trap to eliminate the toluene vapors. The reaction was allowed to continue till the evolution of gas had stopped. The volume of the water displaced by the H_2 gas was recorded. This experiment was repeated three times to get reasonable concordant readings, and the amount of H_2 gas evolved was calculated using the formula given below:

$$n\mathrm{H}_2 = \frac{P(\mathrm{atm}) - P(\mathrm{water}) \times V}{RT} = 1.783\ \mathrm{mmol}\ (\mathrm{expected\ value} = 2.000\ \mathrm{mmol})$$

where $n\mathrm{H}_2$ is the number of moles of H_2 gas produced; P(atm) is atmospheric pressure = 760 Torr; P(water) is vapour pressure of water at 298 K = 23.8 Torr; V is the volume of water displaced = 45.7 mL; R = 62.3635 L Torr K^{-1} mol^{-1}; and T = 298 K.

^1H NMR spectral data for some of the representative products

Butyronitrile. ^1H NMR spectrum (400 MHz, $CDCl_3$, 25 °C) δ (ppm): 2.21 (t, J = 7.5 Hz, 2H), 1.71–1.66 (m, 2H), 0.98 (t, J = 7.4 Hz, 3H).

Octanenitrile. ^1H NMR spectrum (400 MHz, $CDCl_3$, 25 °C) δ (ppm): 2.34 (t, J = 7.1 Hz, 2H), 1.69–1.63 (m, 3H), 1.44 (dd, J = 14.4, 6.7 Hz, 2H), 1.31 (d, J = 8.5 Hz, 8H).

2-Morpholinoacetonitrile. ^1H NMR spectrum (400 MHz, $CDCl_3$, 25 °C) δ (ppm): 3.75 (s, 2H), 3.68 (t, J = 6.0 Hz, 4H), 2.59 (t, J = 7.0 Hz, 4H).

2-Phenoxyacetonitrile. ^1H NMR spectrum (400 MHz, $CDCl_3$, 25 °C) δ (ppm): 7.21 (m, 1H), 7.07 (t, J = 7.8 Hz, 2H), 6.94 (d, J = 8.2 Hz, 2H), 3.91 (s, 2H).

Benzonitrile. ^1H NMR spectrum (400 MHz, $CDCl_3$, 25 °C) δ (ppm): 7.66 (d, J = 7.2 Hz, 2H), 7.61 (t, J = 7.6 Hz, 1H), 7.48 (t, J = 7.7 Hz, 2H).

4-Methylbenzonitrile. ^1H NMR spectrum (400 MHz, $CDCl_3$, 25 °C) δ (ppm): 7.54 (d, J = 8.1 Hz, 2H), 7.27 (d, J = 8.0 Hz, 2H), 2.42 (s, 3H).

2-Aminobenzonitrile. ^1H NMR spectrum (400 MHz, $CDCl_3$, 25 °C) δ (ppm): 7.38 (d, J = 7.9 Hz, 1H), 7.33 (t, J = 7.8 Hz, 1H), 6.73 (dd, J = 7.7, 5.5 Hz, 2H), 4.41 (s, 2H).

4-Aminobenzonitrile. ^{1}H NMR spectrum (400 MHz, $CDCl_3$, 25 °C) δ (ppm): 7.40 (d, J = 8.7 Hz, 2H), 6.63 (d, J = 8.7 Hz, 2H), 4.14 (s, 2H).

2-Hydroxybenzonitrile. ^{1}H NMR spectrum (400 MHz, $CDCl_3$, 25 °C) δ (ppm): 7.49 (dd, J = 16.1, 7.7 Hz, 1H), 7.04–6.96 (m, 1H).

4-Nitrobenzonitrile. ^{1}H NMR spectrum (400 MHz, $CDCl_3$, 25 °C) δ (ppm): 8.81 (d, J = 6.3 Hz, 2H), 7.53 (d, J = 6.3 Hz, 2H).

4-Chlorobenzonitrile. ^{1}H NMR spectrum (400 MHz, $CDCl_3$, 25 °C) δ (ppm): 7.61 (d, J = 8.4 Hz, 1H), 7.47 (d, J = 8.3 Hz, 1H).

2-Chlorobenzonitrile. ^{1}H NMR spectrum (400 MHz, $CDCl_3$, 25 °C) δ (ppm): 7.67 (dd, J = 7.2, 1.5 Hz, 1H), 7.56–7.49 (m, 2H), 7.39–7.34 (m, 1H).

3-Fluorobenzonitrile. ^{1}H NMR spectrum (400 MHz, $CDCl_3$, 25 °C): δ (ppm) 7.69–7.58 (m, 2H), 7.28 (d, J = 8.3 Hz, 1H), 7.25–7.19 (m, 1H).

4-Bromobenzonitrile. ^{1}H NMR spectrum (400 MHz, $CDCl_3$, 25 °C) δ (ppm): 8.35 (d, J = 8.9 Hz), 7.87 (d, J = 8.9 Hz).

3-Bromobenzonitrile. ^{1}H NMR spectrum (400 MHz, $CDCl_3$, 25 °C) δ (ppm): 7.67 (s, 1H), 7.61 (s, 1H), 7.48 (t, J = 7.7 Hz, 2H).

Picolinonitrile. ^{1}H NMR spectrum (400 MHz, $CDCl_3$, 25 °C) δ (ppm): 7.67 (dd, J = 7.7, 1.0 Hz, 1H), 7.53 (dd, J = 6.8, 1.5 Hz, 2H), 7.39–7.33 (m, 1H).

Nicotinonitrile. ^{1}H NMR spectrum (400 MHz, $CDCl_3$, 25 °C) δ (ppm): 8.73 (s, 1H), 7.84 (t, J = 6.9 Hz, 1H), 7.70 (d, J = 7.8 Hz, 1H), 7.52 (dd, J = 7.8, 3.6 Hz, 1H).

Isonicotinonitrile. ^{1}H NMR spectrum (400 MHz, $CDCl_3$, 25 °C) δ (ppm): 8.81 (d, J = 2.7 Hz, 2H), 7.53 (d, J = 2.7 Hz, 2H).

1-Naphthonitrile. ^{1}H NMR spectrum (400 MHz, $CDCl_3$, 25 °C) δ (ppm): 8.12 (d, J = 8.4 Hz), 7.88 (d, J = 7.8 Hz), 7.81 (d, J = 8.2 Hz), 7.58–7.49 (m), 7.47–7.42 (m).

***N*-(Pyridin-2-yl)methanimine.** ^{1}H NMR spectrum (400 MHz, $CDCl_3$, 25 °C) δ (ppm): 8.09 (d, J = 4.1 Hz, 1H), 7.43 (t, J = 6.9 Hz, 1H), 6.63–6.52 (m, 1H), 6.39 (d, J = 8.4 Hz, 1H), 2.93 (s, 2H).

***N*-(Pyridin-4-yl)methanimine.** ^{1}H NMR spectrum (400 MHz, $CDCl_3$, 25 °C) δ (ppm): 8.18 (d, J = 6.4 Hz, 2H), 6.42 (d, J = 6.4 Hz, 2H), 2.86 (s, 2H).

***N*-Benzyl-1-phenylmethanimine.** ^{1}H NMR spectrum (400 MHz, $CDCl_3$, 25 °C) δ (ppm): 7.26 (d, J = 1.8 Hz, 2H), 7.22 (d, J = 1.8 Hz, 2H), 7.09 (d, J = 1.8 Hz, 4H), 6.97 (s, 2H), 6.95 (s, 1H), 3.93 (s, 2H).

Job's plot

Stock solutions of an identical concentration (1 mM) of complex **2** and benzylamine (substrate) were prepared in MeOH. The absorbance in each case, with different complex-substrate ratios but equal volume was recorded. The Job's plot was drawn by plotting the intensity *vs.* mole fraction of benzylamine.

Physical measurements

Elemental analysis data were obtained by the Elementar Analysen Systeme GmbH Vario EL-III instrument. The ^{1}H and ^{13}C NMR spectra were recorded with a JEOL 400 MHz instrument. The FTIR spectra were recorded with an Agilent Cary-630 spectrometer having a diamond ATR. The conductivity measurements were done with an Eutech Instruments conductivity bridge (model: Con-510). The absorption spectra were recorded with a PerkinElmer Lambda-950 spectrophotometer. ESI^+ mass spectra were measured with an Agilent Q-TOF LC-MS mass spectrometer. The cyclic voltametric experiments were conducted on the CH Instruments electrochemical analyzer (model 1120 A). The cell contained a glassy–carbon working electrode, a platinum wire auxiliary electrode, and an Ag/Ag^+ reference electrode.[42,43] The stock solutions were *ca.* 1 mM in Ru(II) complex and 0.1 M in supporting electrolyte, tetrabutylammonium perchlorate.

X-ray crystallography

The X-ray intensity data for complexes **2** and **3** were collected at 273 K with an Oxford XCalibur CCD diffractometer equipped with a graphite monochromatic Mo-Kα radiation (λ = 0.71073 Å).[44] Data reduction was performed with the CrysAllisPro program (Oxford Diffraction ver. 171.34.40).[23] The structures were solved by the direct methods using the SHELXL program and refined on F^2 using all data by full-matrix least-squares procedures with SHELXL-2018/3.[45] The hydrogen atoms were placed at the calculated positions and included in the last cycles of the refinement.[46] For complex **3**, restrain command DELU was applied to obtain reasonable thermal parameters. For both complexes **2** and **3**, some disordered electron density could not be resolved, and therefore, the solvent masking procedure (PLATON SQUEEZE) was used.[47] The electron counts of 36 (two methanol) and 67 (three methanol and one water) were recovered for complexes **2** and **3**, respectively. Such solvent molecules have been included in both the empirical formula and formula weight of complexes. All calculations were done using the WinGX crystallographic software package.[45,47] The crystallographic data collection and structure solution parameters are summarized in Table S1 (ESI).†

Molecular docking studies

The molecular docking studies were performed by using the CIF file of the structurally characterized complex **2** and an energy-minimized chemical drawing of benzylamine using Hex 8.0.0 software.[48] The binding affinity of the metal complex was calculated against the receptor molecule of benzylamine. The binding interactions (docking images) were visualized in Mercury 4.2.0 (Build 257471).

Data availability

The data related to this manuscript are available in the manuscript, as well as the ESI.†

Conflicts of interest

There are no conflicts to declare.

Acknowledgements

RG gratefully acknowledges financial support from the Institution of Eminence, University of Delhi. SY thanks CSIR, New Delhi for her SRF. The authors thank the USIC of this university for the instrumental facilities. Reviewers' comments were very helpful in the revision stage.

References

1 F. F. Fleming, L. Yao, P. C. Ravikumar, L. Funk and B. C. Shook, *J. Med. Chem.*, 2010, **53**, 7902–7917.
2 D. Srimani, M. Feller, Y. Ben-David and D. Milstein, *Chem. Commun.*, 2012, **48**, 11853–11855.
3 K.-N. T. Tseng, A. M. Rizzi and N. K. Szymczak, *J. Am. Chem. Soc.*, 2013, **135**, 16352–16355.
4 H. Tian, C.-Y. Ding, R.-Z. Liao, M. Li and C. Tang, *J. Am. Chem. Soc.*, 2024, **146**, 11801–11810.
5 K. Yamaguchi, H. Fujiwara, Y. Ogasawara, M. Kotani and N. Mizuno, *Angew. Chem., Int. Ed.*, 2007, **46**, 3922–3925.
6 K. Ishihara, Y. Furuya and H. Yamamoto, *Angew. Chem.*, 2002, **114**, 3109–3112.
7 S. S. Moirangthem, D. Ahanthem, S. D. Khongbantabam and W. S. Laitonjam, *ACS Omega*, 2022, **7**, 31348–31351.
8 A. Falk, A.-L. Göderz and H.-G. Schmalz, *Angew. Chem., Int. Ed.*, 2013, **52**, 1576–1580.
9 T. Achard, J. Egly, M. Sigrist, A. Maisse-François and S. Bellemin-Laponnaz, *Chem. – Eur. J.*, 2019, **25**, 13271–13274.
10 M. Kannan, P. Barteja, P. Devi and S. Muthaiah, *J. Catal.*, 2020, **386**, 1–11.
11 W. P. Griffith, B. Reddy, A. G. F. Shoair, M. Suriaatmaja, A. J. P. White and D. J. Williams, *J. Chem. Soc., Dalton Trans.*, 1998, 2819–2826.
12 S. Aiki, A. Taketoshi, J. Kuwabara, T. Koizumi and T. Kanbara, *J. Organomet. Chem.*, 2011, **696**, 1301–1304.
13 J. Kim and S. S. Stahl, *ACS Catal.*, 2013, **3**, 1652–1656.
14 I. Dutta, S. Yadav, A. Sarbajna, S. De, M. Hölscher, W. Leitner and J. K. Bera, *J. Am. Chem. Soc.*, 2018, **140**, 8662–8666.
15 M. Olivares, P. Knörr and M. Albrecht, *Dalton Trans.*, 2020, **49**, 1981–1991.
16 S. Hazra, P. Pilania, M. Deb, A. K. Kushawaha and A. J. Elias, *Chem. – Eur. J.*, 2018, **24**, 15766–15771.
17 S. Budweg, K. Junge and M. Beller, *Catal. Sci. Technol.*, 2020, **10**, 3825–3842.
18 L. V. A. Hale, T. Malakar, K.-N. T. Tseng, P. M. Zimmerman, A. Paul and N. K. Szymczak, *ACS Catal.*, 2016, **6**, 4799–4813.
19 W. H. Bernskoetter and M. Brookhart, *Organometallics*, 2008, **27**, 2036–2045.
20 X. Nie, Y. Zheng, L. Ji, H. Fu, H. Chen and R. Li, *J. Catal.*, 2020, **391**, 378–385.
21 J. P. Shanahan, D. M. Mullis, M. Zeller and N. K. Szymczak, *J. Am. Chem. Soc.*, 2020, **142**, 8809–8817.
22 R. Mitsuhashi, Y. Imai, T. Suzuki and Y. Hayashi, *Molecules*, 2022, **27**, 2098.
23 K. Nakamoto, *in Handbook of Vibrational Spectroscopy*, John Wiley & Sons, Ltd, 2006.
24 Z. Almodares, S. J. Lucas, B. D. Crossley, A. M. Basri, C. M. Pask, A. J. Hebden, R. M. Phillips and P. C. McGowan, *Inorg. Chem.*, 2014, **53**, 727–736.
25 S. Panda, A. Singha Hazari, M. Gogia and G. K. Lahiri, *Inorg. Chem.*, 2020, **59**, 1355–1363.
26 S. Nag, R. J. Butcher and S. Bhattacharya, *Eur. J. Inorg. Chem.*, 2007, **2007**, 1251–1260.
27 M. Maji and S. Kundu, *Dalton Trans.*, 2019, **48**, 17479–17487.
28 B. Procacci, S. B. Duckett, M. W. George, M. W. D. Hanson-Heine, R. Horvath, R. N. Perutz, X.-Z. Sun, K. Q. Vuong and J. A. Welch, *Organometallics*, 2018, **37**, 855–868.
29 P. Vijayan, S. Yadav, S. Yadav and R. Gupta, *Inorg. Chim. Acta*, 2020, **502**, 119285.
30 S. Yadav, P. Vijayan, S. Yadav and R. Gupta, *Dalton Trans.*, 2021, **50**, 3269–3279.
31 S. M. Ashraf, W. Kandioller, M.-G. Mendoza-Ferri, A. A. Nazarov, C. G. Hartinger and B. K. Keppler, *Chem. Biodiversity*, 2008, **5**, 2060–2066.
32 C. Gunanathan and D. Milstein, *Chem. Rev.*, 2014, **114**, 12024–12087.
33 B. Das, A. Rahaman, A. Shatskiy, O. Verho, M. D. Kärkäs and B. Åkermark, *Acc. Chem. Res.*, 2021, **54**, 3326–3337.
34 X.-H. Yang, K. Wang, S.-F. Zhu, J.-H. Xie and Q.-L. Zhou, *J. Am. Chem. Soc.*, 2014, **136**, 17426–17429.
35 B. Karimi, O. Yari, M. Khorasani, H. Vali and F. Mansouri, *ChemCatChem*, 2018, **10**, 1783–1787.
36 D. Ventura-Espinosa, A. Marzá-Beltrán and J. A. Mata, *Chem. – Eur. J.*, 2016, **22**, 17758–17766.
37 S. Pachisia, R. Kishan, S. Yadav and R. Gupta, *Inorg. Chem.*, 2021, **60**, 2009–2022.
38 D. Prabha, S. Pachisia and R. Gupta, *Inorg. Chem. Front.*, 2021, **8**, 1599–1609.
39 S. Yadav and R. Gupta, *Inorg. Chem.*, 2022, **61**, 15463–15474.
40 A. W. Ghoorah, M.-D. Devignes, M. Smaïl-Tabbone and D. W. Ritchie, *Proteins: Struct., Funct., Bioinf.*, 2013, **81**, 2150–2158.
41 D. D. Perrin, W. L. F. Armarego and D. R. Perrin, *Purification of Laboratory Chemicals*, Pergamon Press, Oxford, UK, 1980.
42 A. Brajter-Toth, *J. Am. Chem. Soc.*, 1996, **118**, 10339–10340.
43 N. G. Connelly and W. E. Geiger, *Chem. Rev.*, 1996, **96**, 877–910.
44 *CrysAlisPro, v. 1.171.33.49b*, Oxford Diffraction Ltd., Abingdon, 2009.
45 G. M. Sheldrick, *Acta Crystallogr., Sect. A: Found. Crystallogr.*, 2008, **64**, 112–122.
46 L. J. Farrugia, *J. Appl. Crystallogr.*, 2012, **45**, 849–854.
47 A. L. Spek, *PLATON, A Multipurpose Crystallographic Tool*, Utrecht University, The Netherlands, 2002.
48 D. W. Ritchie, *Hex*, Inria, 2012. **https://hex.loria.fr/**.

